EGFR is a transducer of the urokinase receptor initiated signal that is required for in vivo growth of a human carcinoma

David Liu, Julio A. Aguirre Ghiso, Yeriel Estrada, and Liliana Ossowski[1]

Department of Medicine, Division of Medical Oncology, Mount Sinai School of Medicine, New York, New York 10029
[1]Correspondence: liliana.ossowski@mssm.edu

Summary

Urokinase plasminogen activator receptor (uPAR) activates α5β1 integrin and ERK signaling, inducing in vivo proliferation of HEp3 human carcinoma. Here we demonstrate that EGFR mediates the uPAR/integrin/fibronectin (FN) induced growth pathway. Its activation is ligand-independent and does not require high EGFR, but does require high uPAR expression. Only when uPAR level is constitutively elevated does EGFR become α5β1-associated and activated. Domain 1 of uPAR is crucial for EGFR activation, and FAK links integrin and EGFR signaling. Inhibition of EGFR kinase blocks uPAR induced signal to ERK, implicating EGFR as an important effector of the pathway. Disruption of uPAR or EGFR signaling reduces HEp3 proliferation in vivo. These findings unveil a mechanism whereby uPAR subverts ligand-regulated EGFR signaling, providing cancer cells with proliferative advantage.

Introduction

Mechanisms responsible for elaboration of growth-stimulating signals and molecular events responsible for their sensing are deregulated in cancer cells. In normal cells, activation of MAPK-ERK and growth stimulation require a functional collaboration between secreted growth factor(s) and adhesion-dependent signaling events (Giancotti and Ruoslahti, 1999). Integrins can activate ERK through their α subunit using caveolin and Shc (Wary et al., 1998), and/or through the β subunit and focal adhesion kinase (FAK) (Keely et al., 1998; Cary and Guan, 1999; Giancotti and Ruoslahti, 1999). Potentiation by integrins of growth factor-induced ERK activation is most evident when the integrins are aggregated and bound by ligand (Miyamoto et al., 1996). There is evidence to suggest that clustering of integrins leads to clustering of EGFR and its crossphosphorylation (Miyamoto et al., 1996), and that the process involves FAK-dependent signaling (Sieg et al., 2000). Cooperation between integrins and EGFR in normal cell signaling is further supported by evidence that, even in absence of EGF, EGFR can become activated, leading to activation of ERK, increased cell survival, and partial (G_1/S) traversal of the cell cycle (Moro et al., 1998). This is accomplished through a physical interaction between α5β1 integrins and EGFR, and it occurs in cells with relatively high EGFR expression (Moro et al., 1998). However, even under these conditions, exogenous growth factors are necessary to cause cell progression through G2/M (Moro et al., 1998). Because of their heterogeneity, there is less understanding of the role of integrin and EGFR signaling in proliferation of tumor cells in culture, and the impetus for their in vivo proliferation is even less well understood. It is thought that tumor cells in culture elaborate their own growth factors, including EGFR ligands (Schlessinger, 2000), and use them in an autocrine fashion, but that their dependence for growth on integrin-mediated adhesion and signaling is either unnecessary or dispensable (Ruoslahti, 1999). However, these conclusions were mainly derived from the study of cells grown in agar or as monolayers, i.e., under conditions that do not mimic those existing in vivo, where cells are organized in three-dimensional structures which receive, and must interpret and integrate, multiple signals (Bissell et al., 1999).

We previously showed that highly malignant human carcinoma T-HEp3 cells grow rapidly in vivo, and have a very high level of active ERK (Aguirre Ghiso et al., 1999). This activity was dependent on high expression of urokinase receptor (uPAR). The fact that there is substantial published evidence to document overexpression of uPAR in most malignant cancers and to show that its expression is a predictor of poor prognosis in cancer (for review see Andreasen et al., 1997; Schmitt et al., 2000) underscores the relevance of our finding. We found that the overexpressed uPAR interacted with and activated α5β1-integrin. This activation was maximal when uPAR was bound to uPA and α5β1 to FN. In HEp3 cells in which the level of uPAR was diminished by prolonged culture (D-HEp3), or by stable

SIGNIFICANCE

Cancer cells notoriously evade host-imposed growth inhibition, often by constitutively activating autocrine growth pathways or overexpressing surface receptors. We identified a mitogenic pathway whereby a squamous carcinoma with overexpressed urokinase receptor (uPAR) and a normal level of EGFR utilizes uPAR to activate a ligand-independent EGFR signal in vivo. This is important in view of current clinical trials utilizing antibody blockade of ligand binding to EGFR. Since many malignant tumors overexpress uPAR, they may stimulate EGFR signaling in spite of normal EGFR levels and absent ligand-producing capacity. Patients with such tumors may fail on anti-EGFR antibody therapy, requiring interventions that consider the role of uPAR in promoting tumor growth. Our characterization of uPAR-dependent steps that culminate in tumor growth may provide opportunities for therapeutic interventions.

transfection with a plasmid expressing uPAR-antisense (AS24), fewer uPAR/α5β1 complexes were formed and the signal to ERK was reduced to the level that allowed their in vivo survival but precluded growth, forcing them into a state of dormancy (Yu et al., 1997; Aguirre Ghiso et al., 1999). Because integrin-induced activation of EGFR has been linked in some cells to EGFR overexpression (Moro et al., 1998), and since HEp3 cells are derived from a head and neck tumor known to overexpress this growth factor receptor (Nicholson et al., 2001), we wondered what role, if any, EGFR played in ERK activation and growth of these cells. Preliminary data showed that, contrary to the expected, D-HEp3 cells expressed much higher EGFR levels than T-HEp3 cells, but the receptor was not phosphorylated. This suggested that the mere presence of α5β1 integrin and high levels of EGFR, thought to be sufficient for EGFR activation upon adhesion to FN (Moro et al., 1998), may not be adequate to induce receptor activation and proliferation in all cell types. Our previous work indicated that T-HEp3 cells are highly dependent on FN-generated, uPAR/integrin-transduced signals for their in vivo growth (Aguirre Ghiso et al., 1999, 2001). Here we provide novel information that strongly implicates uPAR in regulation of EGFR activity in culture and, most importantly, in vivo. Our data identify EGFR as the mediator of signals initiated by the uPA/uPAR/FN/α5β1 complex that result in the very high and persistent level of ERK activity necessary for the in vivo growth of HEp3 cancer cells.

Results

We previously linked high uPAR expression to its frequent interactions with α5β1-integrin, high ERK activity, and in vivo growth of T-HEp3 cells (Aguirre Ghiso et al., 1999). Because ERK is also a downstream effector of both integrins and EGFR, we have now investigated the potential role of this growth factor receptor in the chain of events leading from high uPAR expression to T-HEp3 tumorigenicity.

Level of EGFR expression and its state of activation

We assayed EGFR in lysates of uPAR-rich tumorigenic HEp3 (T-HEp3 and LK25) cells and uPAR-poor, dormant HEp3 (D-HEp3 and AS24) cells by Western blotting. We found a 5-fold greater EGFR-protein content in D-HEp3 and AS24 cells (Figures 1A and 1F), and this result was corroborated by FACS analysis of surface expression of EGFR (Figure 1B). This finding was surprising, because EGFR overexpression is known to result in its autophosphorylation and signaling (Schlessinger, 2000), and our previous results showed that ERK activity was very low in D-HEp3 cells (Aguirre Ghiso et al., 1999). We then monitored EGFR autophosphorylation in serum-starved T-HEp3 and D-HEp3 cells using direct Western blotting with antiactive EGFR antibodies (Figure 1C) or EGFR immunoprecipitation followed by Western blotting with antiphosphotyrosine antibodies (Figure 1D). In spite of their low EGFR content but in agreement with their high ERK activity, we found a 7- to 10-fold greater level of phospho-EGFR in T-HEp3 cells. Published data indicate that EGFR becomes tyrosine-phosphorylated when cells expressing α5β1 integrin and abundant EGFR are allowed to adhere to FN (Moro et al., 1998). Therefore, we tested the effect this treatment had on EGFR activation in T-HEp3 and D-HEp3 cells; adhesion to poly-L-lysine (PLL) served as a negative control. We found that the level of phospho-EGFR was higher in unstimulated (adherent to PLL) T-HEp3. More importantly, a strong stimulation was observed only in these cells, after adhesion to FN (Figure 1E). Similar results were obtained when LK25 and AS24 cells were compared (Figure 1F). Thus, it appears that it is the uPAR, and not the α5β1 integrin presence or EGFR level, that determine its activation. Since each of the cell types examined expresses similar levels of α5β1-integrin (Aguirre Ghiso et al., 1999, 2001), and since EGFR becomes tyrosine-phosphorylated upon cell adhesion to FN only in T-HEp3 and LK25 cells, which have low EGFR levels, we had to assume that mechanisms other than EGFR overexpression, possibly involving an autocrine loop, must be responsible for its activation.

We compared the expression of known EGFR-ligands EGF, TGFα, β-cellulin, HB-EGF, and amphiregulin in T- and D-HEp3 cells. We found that the expression of EGF, β-cellulin, and amphiregulin was undetectable even by RT-PCR, and TGFα was detectable only by PCR and only in D-HEp3 cells, while HB-EGF, detectable by both RT-PCR (results not shown) and Northern blot, was similarly expressed in D- and T-HEp3 cells (Figure 2B). To rule out the possibility that it was not the overall level of HB-EGF but the ability of T-HEp3 cells to process it to a mature form (Goishi et al., 1995) that was responsible for EGFR activation, we tested the effect of medium conditioned by T-HEp3 cells on the EGFR and ERK activation in D-HEp3 cells. While treatment of D-HEp3 cells with 20 ng/ml EGF induced both EGFR and ERK phosphorylation, indicating that the receptor and the signaling pathway were intact, T-HEp3 conditioned medium was ineffective (Figure 2C). In addition, exogenous HB-EGF stimulated EGFR phosphorylation in T-HEp3, and this stimulation was sensitive to inhibition by CRM197 (a mutant diphtheria toxin that blocks mitogenic activity of HB-EGF) (Mitamura et al., 1995) (Figure 2D). In contrast, neither the basal EGFR phosphorylation nor the phosphorylation induced by adhesion to FN was affected by CRM197 (Figures 2D and 2E).

Overall, these results show that in HEp3 cells, EGFR activation is independent of an autocrine loop, and that α5β1-integrin and high EGFR expression is not sufficient for FN-induced EGFR activation. The results also show a correlation between EGFR-activation and uPAR expression.

Effect of uPAR on α5β1-EGFR interaction and EGFR signaling

To consider the role of uPAR in the regulation of EGFR activation and the involvement of integrins in this process, we first explored whether there was a physical interaction between α5β1 and EGFR and whether this interaction was uPAR-dependent. T- and D-HEp3 cell lysates were immunoprecipitated either with anti-β1 (Figure 3A) or anti-EGFR (Figure 3B) antibodies and blotted with anti-β1 and anti-EGFR antibodies, respectively. Although T-HEp3 and D-HEp3 cells contain a similar amount of β1 integrin, EGFR was associated with β1 only in uPAR-rich T-HEp3 cells. In a parallel experiment, anti-EGFR antibodies pulled down much more EGFR from the D-HEp3 cells, but the relative amount of coimmunoprecipitated β1 integrin was much smaller than in T-HEp3 cells (Figure 3B). Similar results were obtained when LK25 and AS24 cells, plated on FN and then lysed, were immunoprecipitated with anti-α5β1 antibody. Thus, more EGFR was associated with α5β1 integrin in uPAR-rich LK25 cells. More importantly, in LK25 cells, EGFR present in the complex with integrin was phosphorylated (Figure 3C), whereas no phosphorylated population was detectable in AS24

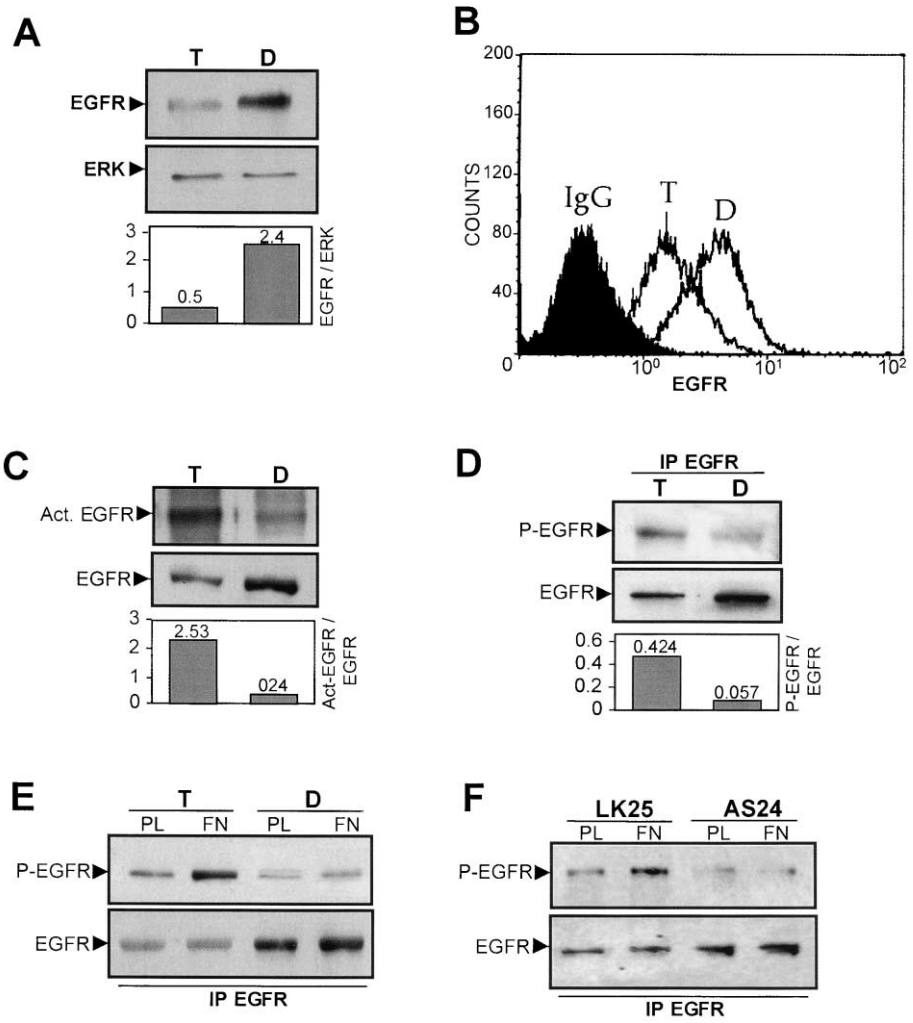

Figure 1. EGFR content, state of activation, and effect of cell binding to FN in uPAR-rich and uPAR-deficient HEp3 cells

A: Cell lysates from serum-starved T-HEp3 (T) and D-HEp3 (D) cells, immunoblotted with polyclonal EGFR antibody (top) for total EGFR content and anti-ERK (MK12) antibody for loading control (bottom). The graph shows EGFR/ERK ratio obtained by densitometric scanning (see Experimental Procedures).

B: Surface expression of EGFR was measured using FACS® analysis as described in Experimental Procedures.

C: Cell lysates from serum-starved T-HEp3 (T) and D-HEp3 (D) cells were immunoblotted for active-EGFR (mAb 74, top) and total EGFR (polyclonal anti-EGFR, bottom). Active-EGFR/EGFR ratio was determined as in **A** (graph).

D: EGFR was immunoprecipitated from 800 μg of T-HEp3(T) and D-HEp3(D) NP-40 buffer cell lysate protein (see Experimental Procedures) using mouse anti-EGFR antibody (mAb 225, 3 μg), and the resulting immunoprecipitates (IP) were analyzed by IB for phosphotyrosine (PY-20, top) or total EGFR (polyclonal anti-EGFR, bottom). The phospho-EGFR (P-EGFR)/total EGFR ratio was obtained as in **A** (graph).

E: T-HEp3 (T) and D-HEp3 (D) were plated on FN (or PLL as negative control) for 20 min. EGFR was immunoprecipitated from 1 mg of cell lysate protein as in **D**, split equally into two aliquots and immunoblotted for phosphotyrosine (RC-20, top) and total EGFR (bottom).

F: As in **E** except comparing LK25 (uPAR-rich) and AS24 (uPAR-deficient) cells.

cells. Additional support for uPAR regulation of EGFR association with α5β1 integrins was obtained from a fibrosarcoma cell line, HT1080, transfected with uPAR-antisense under an inducible promoter. While EGFR was found to be integrin-associated in HT1080 cells expressing uPAR (in presence of tetracycline), upregulation of the antisense by removal of the antibiotic from the incubation medium reduced uPAR level by ~90% and reduced α5β1 integrin-associated EGFR protein to barely detectable levels (results not shown). Taken together, these findings show that it is not the levels of EGFR or the α5β1 integrin, which do not change upon uPAR-antisense induction in HT1080 cells, but the abundance of uPAR that determines EGFR-integrin interaction and EGFR phosphorylation following adhesion to FN.

To confirm this conclusion in intact cells, we used fluorescence confocal microscopy. We have previously shown using this method that most of the surface expressed uPAR colocalized with β1 integrin in T-HEp3 cells (Aguirre Ghiso et al., 2001). We now tested the surface localization of EGFR and β1 integrin in uPAR-rich and uPAR-poor cells using antibodies to β1 and the phosphorylated (active) form of EGFR. The levels and distribution of β1 integrin were similar in T and D-HEp3 cells (Figure 3D, left column). However, while in the D-HEp3 cells the staining of active EGFR was of a very low intensity and was homogeneously distributed in the plasma membrane, in the T-HEp3 cells, the staining of active EGFR was much more intense and was concentrated in focal areas and in cell-cell junctions (Figure 3D, center column). An overlay of the β1 and the active EGFR images showed a high degree of colocalization, suggesting molecular proximity between the integrin and active EGFR (Figure 3D, right column) and supporting the coimmunoprecipitation data (Figures 3A–3C).

Activation of ERK is an important downstream target of active EGFR. To test whether EGFR activated by uPAR signaled to ERK, serum-starved T-HEp3 cells plated on FN, or on PLL as negative control, were examined for phospho-EGFR and phospho-ERK content. As shown in Figure 4A, the increase in phospho-EGFR correlated with increased ERK activity.

Because we had shown earlier that uPAR interaction with α5β1 integrin resulted in a potent ERK activation in T-HEp3 cells (Aguirre Ghiso et al., 1999), we wondered whether ERK activation induced by EGFR and by the uPAR-activated integrins was a result of converging or separate pathways. To test this, we examined the effect of inhibition of EGFR kinase activity on ERK activation by two independent approaches. First, T-HEp3 cells were preincubated for 15 min with or without a pharmacological inhibitor of EGFR-kinase, AG1478, before plating on FN

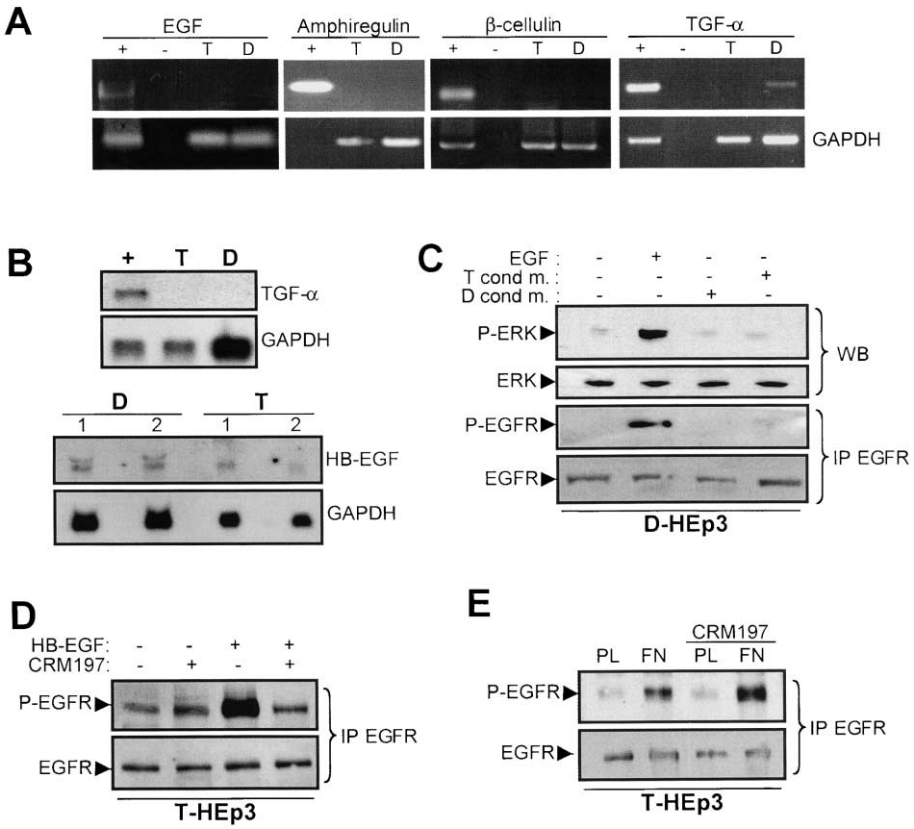

Figure 2. Analysis of expression of EGFR ligands in T and D HEp3 cells

A: RT-PCR analysis for expression EGF, amphiregulin, β-cellulin, and TGF-α (top panels) was performed on total RNA preparations from serum-starved T-HEp3 (T) and D-HEp3 (D) cells. RT-PCR of GAPDH served as loading control (bottom panels). Shown, ethidium bromide stained bands in 1% agarose gel. Positive controls (+): RNA from LnCAP cells for EGF; from MDA231 cells for TGF-α and β-cellulin; 300 bp PCR fragment for amphiregulin. Negative control (−): no RNA template.

B: Northern blot analysis for TGF-α (with positive control RNA from MDA231 cells) and HB-EGF (in duplicate) mRNA. GAPDH used as loading control (top and bottom).

C: D-HEp3 cells, serum-starved for 24 hr, were treated for 20 min with EGF (20 ng/ml), conditioned medium (48 hr in serum-free medium) of D-HEp3 ($D_{cond\ m}$) or T-HEp3 ($T_{cond\ m}$) cells, or fresh medium. Cell lysates (50 μg protein) were blotted for phosphorylated ERK (P-ERK, mAb E-4) and total ERK (top panels). EGFR immunoprecipitated from the same cell lysates (500 μg protein with 5 μg mouse Ab5) was blotted for phospho-EGFR and total EGFR (bottom panels).

D: T-HEp3 cells, serum-starved for 24 hr were treated for 20 min with CRM197 (10 μg/ml) or kept untreated. To ensure specificity, cells were then treated with HB-EGF (20 ng/ml) or medium alone in the presence or absence of CRM197 (10 μg/ml) for 5 min. Immunoprecipitated EGFR was blotted for phosphotyrosine (RC-20, top) and total EGFR (bottom).

E: T-HEp3 cells, serum-starved and treated with CRM197 as in **D**, were plated on FN (or PLL as negative control) for 20 min. EGFR was immunoprecipitated from 1 mg of cell lysate protein as in Figure 1D and analyzed for phosphotyrosine (top) and total EGFR (bottom).

or PLL (Figure 4A) and collecting the cells 20 min later for analysis. As shown in Figure 4A, this inhibitor blocked both the basal and the FN-stimulated EGFR phosphorylation, but only the FN-stimulated ERK phosphorylation was blocked (Figure 4A). This suggests that EGFR kinase activity is required for the propagation of the FN-dependent signal to ERK, and that there is an additional ERK-activating "constitutive" FN-independent pathway of low efficiency that appears to be EGFR independent.

We also used genetic approach whereby T-HEp3 cells were transiently transfected with a C-terminal truncated form of EGFR, CD533 (Spivak-Kroizman et al., 1992; Redemann et al., 1992), which functions as a dominant negative EGFR, presumably by forming heterodimers with the wild-type receptor. The dominant negative mutant was expressed in excess of the native, wild-type EGFR, and it strongly reduced the FN-induced tyrosine phosphorylation of EGFR, suggesting that homodimerization of wt EGFR is required (Figure 4B). This reduction was linked to a similar reduction in phospho-ERK (Figure 4B, lower panel). Together, these results directly implicate EGFR as a downstream effector of uPAR and α5β1 signal transduction that leads to ERK activation in an uPAR-rich environment.

To test the contribution of this pathway to growth in vivo, T-HEp3 cells (5×10^5), pretreated with 1 μM AG1478 for 24 hr under serum-free conditions, or kept in medium alone, were inoculated on to the CAMs of chick embryos. Untreated T-HEp3 cells grew rapidly on the CAM, forming large tumors containing $\sim 10^7$ cells by day 5 (Figure 4C), while the AG1478 pretreated cells formed small tumors in which the cell number was reduced by ~60% on day 5. In a parallel experiment, treatment of T-HEp3 cells with AG1478 (0, 0.5, 1, and 5 μM) for 3 days in culture produced no inhibition of cell growth (results not shown). The result of the in vivo experiment demonstrates that EGFR signaling is required for the full proliferative potential of uPAR-rich T-HEp3.

The mechanism of EGFR activation by uPAR

To test the role of uPAR in EGFR activation directly, uPAR expression was restored in D-HEp3 cells (Figure 5A, insert) to the level found in T-HEp3 cells (Aguirre Ghiso et al., 2001). We previously showed that reexpression of uPAR interrupted the in vivo dormancy of D-HEp3 cells, yielding cells capable of in vivo growth (Aguirre Ghiso et al., 2001). We now tested whether, similar to the parental T-HEp3 cells, these cells utilized uPAR-induced and ligand-independent EGFR activation to generate their mitogenic signals. The results in Figure 5A confirmed that uPAR reexpression restores the in vivo proliferation of these cells. Moreover, while pretreatment with AG1478 reduced their growth in vivo, pretreatment with an EGFR-blocking antibody did not (Figure 5A, top and bottom panels). Thus, it appears that the tumorigenic phenotype restored by uPAR reexpression possesses the hallmarks of the parental T-HEp3 cells. In order to strengthen this conclusion, we tested whether uPAR reexpression induced integrin/EGFR association characteristic of the uPAR-rich T-HEp3 cells (Figure 3). Pools of vector and uPAR

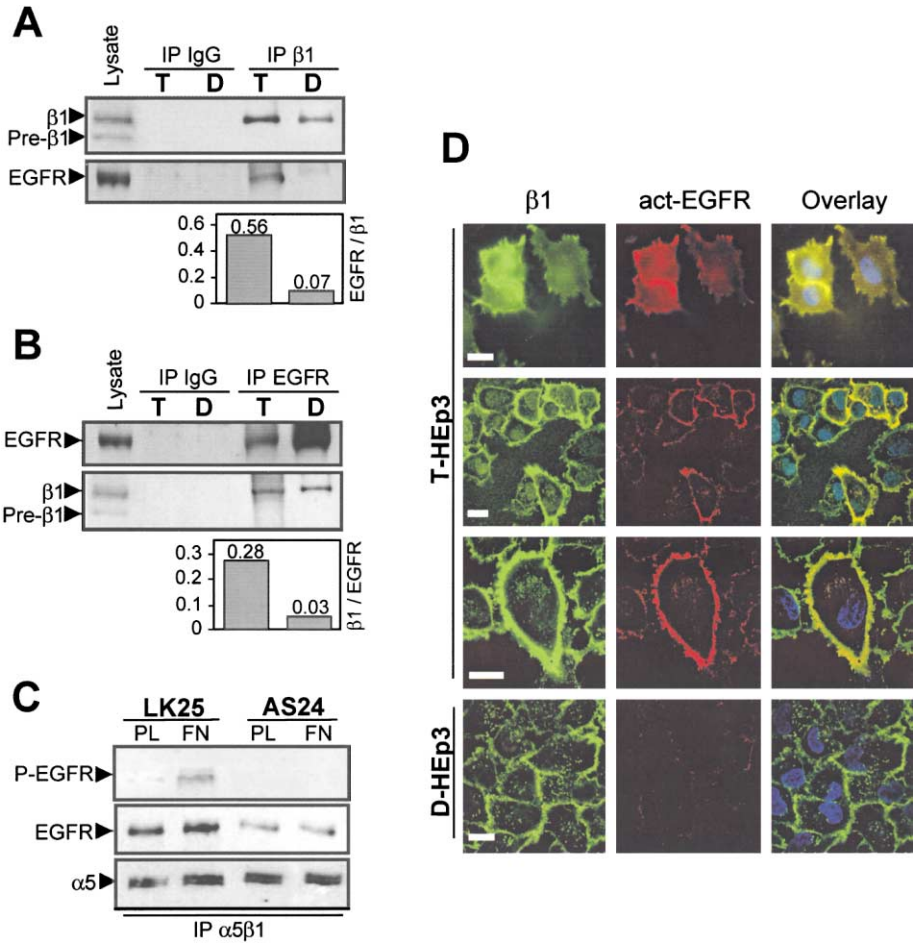

Figure 3. EGFR/α5β1 integrin association and EGFR activation correlates with uPAR expression

A: Cell lysates from serum-starved T-HEp3 (T) and D-HEp3 (D) cells were incubated with anti-β1 antibody (mAb TS2/16, 5 μg) (IP β1) or isotype matched IgG (IP IgG). The immunoprecipitates were blotted for β1 (4B7R, top) and total EGFR (bottom). EGFR/β1 ratio obtained as in Figure 1A (graph). D-HEp3 total protein lysate was blotted as positive control.

B: Same as in **A** except immunoprecipitated with anti-EGFR (mouse Ab5, 5 μg). β1/EGFR ratio obtained as in Figure 1A (graph).

C: LK25 (uPAR-rich) and AS24 (uPAR-deficient) cells were plated on FN or on PLL as negative control for 20 min. α5β1-integrin was immunoprecipitated from 800 μg of cells protein with 5 μg of VLA5 antibody and blotted for phosphotyrosine (RC-20, top) and α5 (polyclonal anti-α5; bottom). Phosphotyrosine blot was stripped and reblotted for total EGFR (middle panel).

D: Colocalization of active EGFR and β1 integrins. T-HEp3 and D-HEp3 were plated on glass coverslips and immunostained for β1 (in green) and activated EGFR (in red; act-EGFR). Overlay is shown in yellow. DAPI stained nuclei are in blue. Active EGFR colocalizes with β1-integrin only in uPAR-rich, T-HEp3 cells.

transfected cells were lysed and immunoprecipitated using anti-β1 antibody and blotted with anti-EGFR and anti-α5 antibodies. The results in Figure 5B (bottom) show that a similar level of the α5 integrin subunit was pulled down with the anti-α5β1 antibody, indicating that there was no major change in the α5β1 integrin level upon uPAR reexpression. However, EGFR was found to be associated with the integrin only in cells that reexpressed uPAR (Figure 5B, top). This result implicated uPAR in regulation of integrin/EGFR interaction. We previously showed that lateral interaction of uPAR with α5β1 leads to integrin activation and function as measured by the ability to assemble FN fibrils (Aguirre Ghiso et al., 2001), phosphorylation of FAK and activation of ras (Aguirre Ghiso, 2002), initiation of an intracellular signal (Aguirre Ghiso et al., 2001), presumably through an "outside-in" mechanism, and, as shown here, activation of EGFR. To further explore the nature of α5β1-integrin activation by uPAR and its effect on EGFR phosphorylation, we compared its effect to the effect of known "outside-in" α5β1-integrin activators, Mn^{2+} and a β1-activating antibody, TS2/16, which increased the binding of ^{125}I-labeled FN to D-HEp3 cells and adhesion of these cells to FN (results not shown and Aguirre Ghiso et al., 1999). As shown in Figures 5C and 5D, both treatments strongly increased FN-induced EGFR-phosphorylation. These results show that, although, under basal conditions, the α5β1-integrin in D-HEp3 cells is inactive, it can be activated by Mn^{2+} or antibody treatment, and that reexpression of uPAR produces a similar effect.

To gain further insight into the structure/function relation of uPAR as an inducer of EGFR activation, we prepared a truncated uPAR lacking domain 1 (D1) (referred to as D2D3), and a mutant in which the protease sensitive sites in the linker peptide between D1 and D2 were mutated (referred to as noncleavable, nc), making it resistant to protease cleavage (Hoyer-Hansen et al., 1992). D-HEp3 cells were transfected, and hygromycin-resistant pools of cells were obtained that expressed the mutant uPAR at levels similar to that obtained for full-length uPAR (Figure 5E). The effect of modification of uPAR structure on the FN-induced EGFR activation was tested. As shown in Figure 5F, left panel, the FN-induced EGFR activation was marked in cells transfected with the wild-type uPAR, and even stronger in cells transfected with the noncleavable uPARnc mutant. Quantitative analysis of 3 experiments (Figure 5F, right panel) confirmed these results and also showed that cell transfected with the mutant missing domain 1 (D2D3) were unable to activate EGFR when plated on FN. This suggests that optimal uPAR-integrin interaction depends on the D1 domain and that uncleaved uPAR is most effective in EGFR activation.

FAK links intracellular signaling of uPAR/integrin and EGFR

The experiments illustrated in Figures 4A and 4B show that pharmacologic and genetic inhibitors of EGFR kinase block

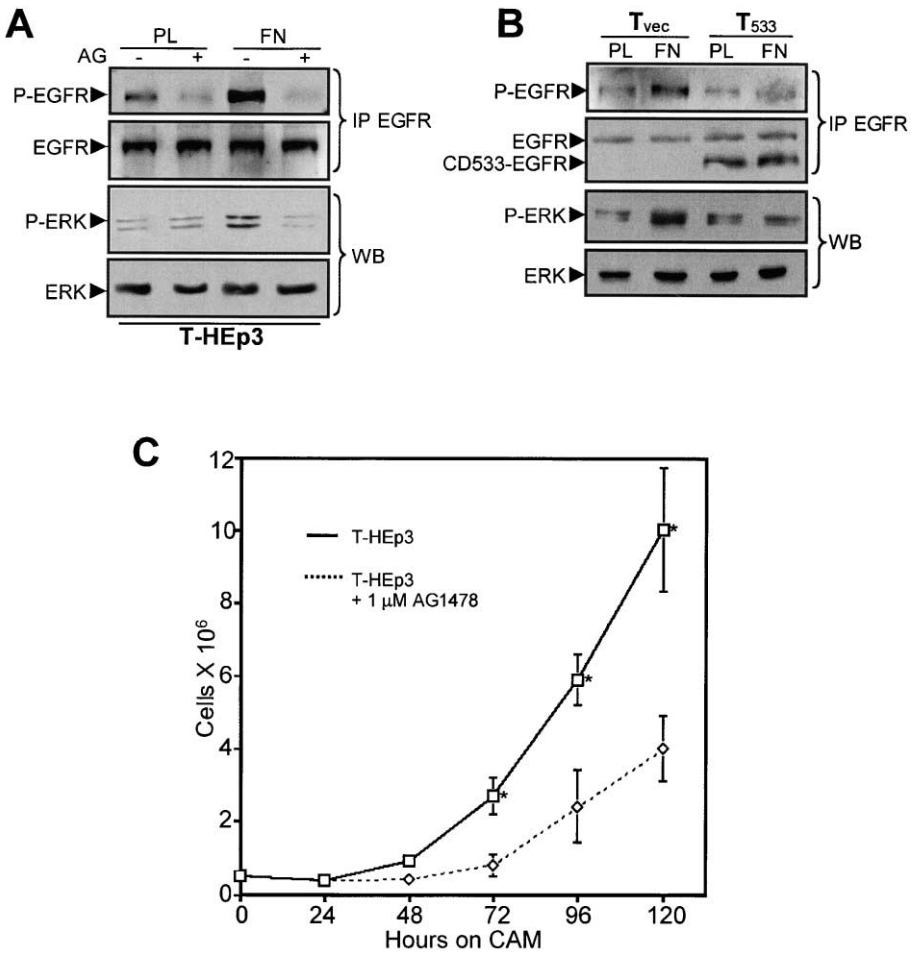

Figure 4. Functional EGFR kinase is required for integrin-mediated EGFR activation and in vivo growth of uPAR-rich HEp3 cells

A: T-HEp3 pretreated with (+) AG1478 (AG) or untreated (−) were plated on FN, or on PLL as negative control, for 20 min. Immunoprecipitated EGFR was blotted for phosphotyrosine (RC-20, top panel) and total EGFR (top panel, bottom). Cell lysate protein was analyzed for P-ERK (third panel) and ERK (bottom panel) by direct IB.

B: T-HEp3 cells transfected with vector (T_{vec}) or with CD533-EGFR (T_{533}) were plated on FN or PLL. Efficiency of transfection of T-HEp3 using a plasmid coding for GFP under the same promoter as the CD533 was determined to be greater than 40%. Immunoprecipitated EGFR was analyzed for P-EGFR (top panel), EGFR (mAb 14; second panel), P-ERK (third panel), and ERK (bottom panel) as in **A**.

C: Growth of T-HEp3 cells pretreated with AG1478, or untreated, on the CAM (see Experimental Procedures). Each point represents the mean ± SE of five samples. *$P < 0.0001$ T-HEp3 control versus T-HEp3 + AG1478 as determined by ANOVA test.

almost entirely the uPAR and FN-induced ERK activation, suggesting that the pathways from integrin and from EGFR to ERK are functionally linked. We previously found that FAK associates with β1-integrin in HEp3 cells (Aguirre Ghiso, 2002). In an attempt to identify the site of crossover between the α5β1-integrin and EGFR pathways, we considered the recently published evidence suggesting that FAK may act as a receptor-proximal bridging protein between growth factor receptors and integrin signaling (Sieg et al., 2000). Specifically, we examined whether the presence of EGFR-FAK association exists in vivo and in culture. T-HEp3 cells (2×10^5) and D-HEp3 cells (1.2×10^6) were inoculated on the chorioallantoic membrane (CAM) of chick embryos and incubated for 7 days. T-HEp3 cells grew into large tumors, while the D-HEp3 cells formed small nodules with little or no increase in cell number, confirming their in vivo dormancy (Ossowski and Reich, 1980; Aguirre Ghiso et al., 1999). One T-HEp3 tumor and ten D-HEp3 nodules were collected in lysis buffer, immunoprecipitated with anti-EGFR antibodies, and blotted for phospho-tyrosine. Unlike in the D-HEp3 cell culture, the total level of EGFR was somewhat lower in the D-HEp3 nodules, most likely due to dilution of the sample with host cell proteins. Nevertheless, it can be seen that the ratio of phospho-EGFR to EGFR was much lower in D-HEp3 nodules than in T-HEp3 CAM tumors (Figure 6A). More importantly, a large number of phosphoproteins were found to coimmunoprecipitate with the EGFR pulled down from the uPAR-rich T-HEp3 tumors. Using specific antibodies, we identified the ~125 kDa phosphoprotein as FAK (Figure 6A, middle panel). We also found that Ras, previously shown to be more active in T-HEp3 cells (Aguirre Ghiso, 2002), was preferentially associated with the EGFR complex in vivo in T-HEp3 cells, suggesting that the Ras-ERK activation signal is initiated by EGFR (results not shown). Although the additional EGFR-associated phosphoproteins are still awaiting identification, it appears that EGFR is part of a large in vivo complex of potential signaling proteins, which is absent from uPAR deficient D-HEp3 cells.

To test the role of FAK in uPAR-mediated EGFR activation, we immunoprecipitated EGFR from T-HEp3 cells, blotted the proteins with anti-phosphotyrosine antibody, and then stripped and blotted for EGFR or FAK. The results show that in uPAR-rich cells, FAK can be coimmunoprecipitated with EGFR, and that the EGFR-associated FAK is phosphorylated, suggesting the requirement for functional FAK (Figure 6B). To determine whether active FAK was required for integrin/EGFR complex assembly or for downstream signaling, T-HEp3 cells were transfected with FRNK, a natural splice variant of FAK that has been shown to displace FAK from integrin association and to block FAK activity in several cell lines (Cary and Guan, 1999; Sieg et al., 2000), including the T-HEp3 cells (Aguirre Ghiso, 2002). The EGFR/integrin association was probed in vector and FRNK-

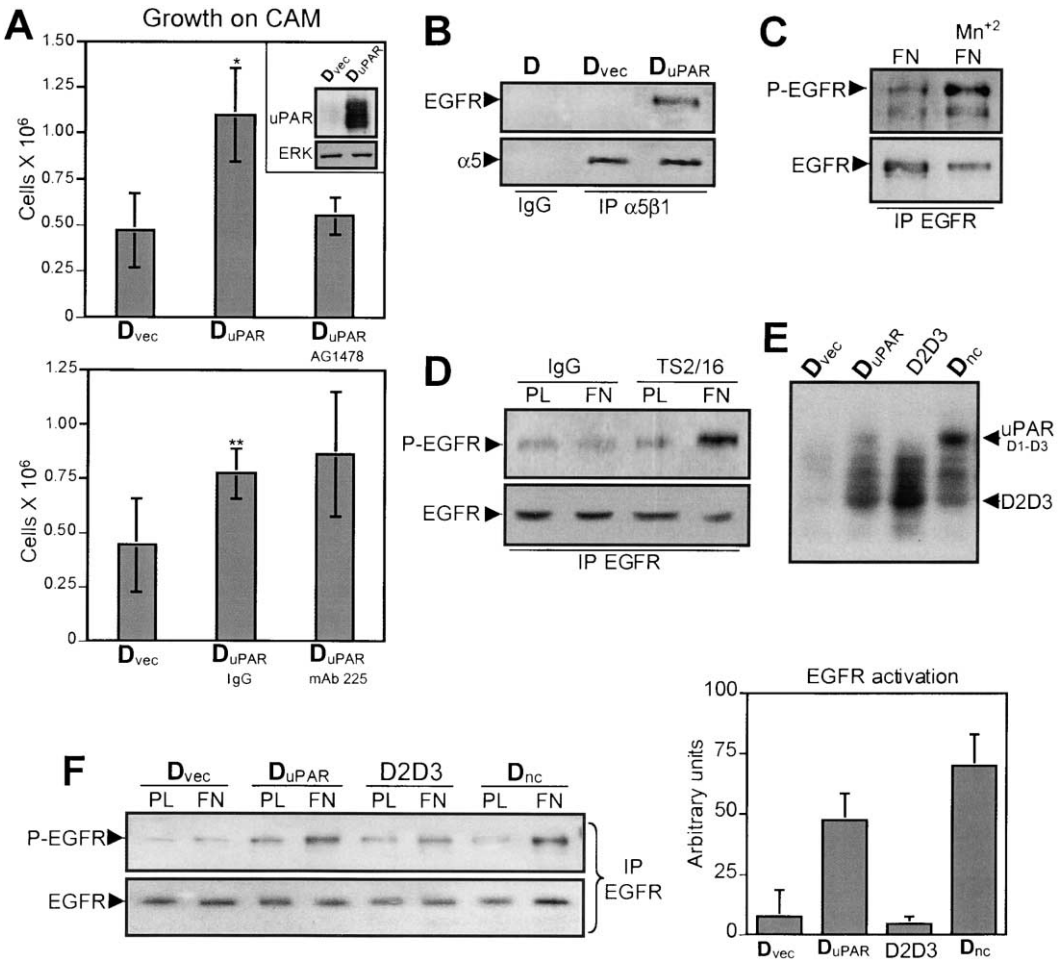

Figure 5. Mechanism of integrin-activation-dependent EGFR stimulation by uPAR

A: D-HEp3 cells transfected with vector (D_{vec}) or wild-type uPAR (D_{uPAR}) pretreated with 1 μM AG1478, or untreated (top graph), or with mAb 225 (IgG as control) (bottom graph) were analyzed for growth after 96 hr on the CAM (see Experimental Procedures). Each bar represents the mean ± SD of five samples. *$P < 0.001$ D_{uPAR} versus D_{uPAR} with AG1478 and **$P < 0.05$ D_{vec} versus D_{uPAR} with IgG as determined by Student's t test. There was no significant difference in D_{uPAR} growth between IgG and mAb 225 treated cells. Expression of the transgene was tested by IB with anti-uPAR antibody (R2) and ERK as loading control (insert).

B: α5β1-integrin was immunoprecipitated from 800 μg of D_{vec} and D_{uPAR} lysate protein with 5 μg of VLA5 antibody and blotted for EGFR (top) and α5 (polyclonal anti-α5; bottom). Isotype-matched IgG was used as control.

C: D-HEp3 cells without or with 1.5 mM $MnCl_2$ were plated on FN (see Experimental Procedures). EGFR was immunoprecipitated from 1 mg of total cell lysate protein as in Figure 1D, split equally into two aliquots, and blotted for phosphotyrosine (RC-20, top) and total EGFR (bottom).

D: D-HEp3 cells treated with anti-β1 activating antibody, TS2/16, or isotype-matched IgG were plated on FN or PLL and processed as in **C** for phosphotyrosine (top) and total EGFR (bottom).

E: D-HEp3 cells transfected with vector (D_{vec}) or vector expressing wild-type uPAR (D_{uPAR}), mutant-D2D3, and noncleavable uPAR (D_{nc}) expressed similar level of the protein, as determined by IB.

F: Transfected cells (see **E**) were plated on FN or PLL and processed as in **C** for phosphotyrosine (top) and total EGFR (bottom). Columns in graph represent mean EGFR activation on FN (minus PLL background) as determined by densitometry of bands from three independent experiments. Error bars represent SEM.

transfected cells by immunoprecipitation of cell lysates with anti-EGFR antibody followed by blotting with anti α5 antibody. The results (Figure 6C) show that expression of FRNK reduced the integrin/EGFR association, suggesting that FAK may be important in complex assembly. The requirement for functional FAK in FN-induced EGFR activation was further examined in vector and FRNK-expressing cell by plating the cells on PLL or FN and blotting for phospho-EGFR in immunoprecipitates of EGFR. While adhesion to FN induced EGFR phosphorylation in vector transfected cells, T-HEp3 cells expressing FRNK failed to activate EGFR when plated on fibronectin (Figure 6D). This result suggests that functional FAK is required for uPAR-mediated activation of EGFR in HEp3 tumor cells and that it may serve to integrate integrin and EGFR signaling even in absence of EGFR ligand.

Dependence of EGFR activation on an intact uPA/uPAR-FN/integrin complex in culture and in vivo

We have previously shown that binding of uPA to uPAR leads to a robust ERK activation (Aguirre Ghiso et al., 1999). To test

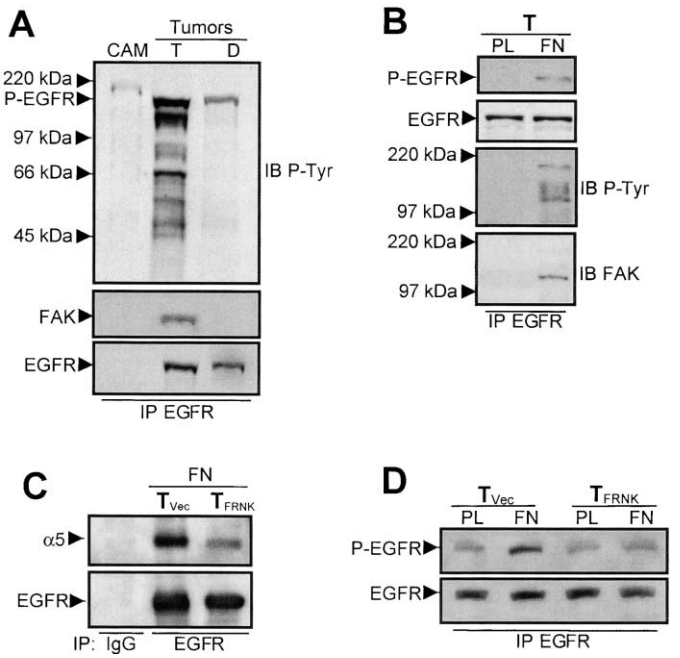

Figure 6. The role of FAK in uPAR-dependent EGFR activation in culture and in vivo

A: T-HEp3 (T) and D-HEp3 (D) cells were inoculated and grown on the CAM for seven days and processed as described in Experimental Procedures. 1.5 mg of protein from whole tumor lysates was immunoprecipitated with anti-EGFR antibody (mAb 225, 3 μg) and blotted for phosphotyrosine (RC-20, top). The membrane was stripped and blotted for total EGFR (bottom), and after additional stripping, blotted for FAK (mAb 77; middle).

B: T-HEp3 (T) cells were plated on FN or on PLL (see Experimental Procedures). EGFR was immunoprecipitated as in Figure 1D, and blotted for phosphotyrosine (RC-20, top and third panel) and total EGFR (second panel). The membrane was reblotted for FAK (bottom panel).

C: T-HEp3 cells transfected with vector (T_{vec}) or vector expressing FRNK (T_{FRNK}) were plated on FN. EGFR was immunoprecipitated from 1 mg of cell lysate protein as in Figure 1D and analyzed for α5 (top) and total EGFR (bottom). Isotype-matched IgG was used as negative control.

D: T_{vec} or T_{FRNK} were plated on FN or PLL (see Experimental Procedures). EGFR and P-EGFR were determined as in **B**.

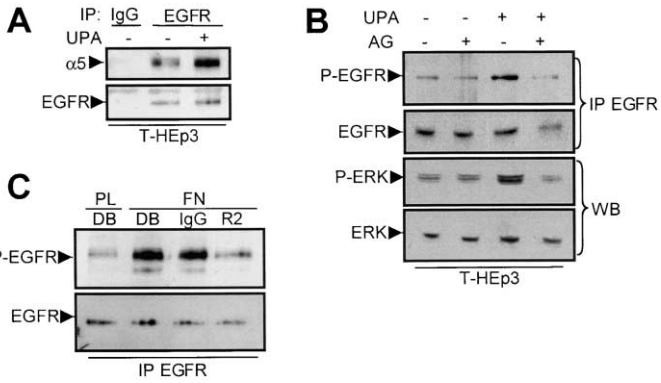

Figure 7. EGFR kinase as a mediator of uPA/uPAR/integrin-induced EGFR signaling to ERK

A: T-HEp3 cells were stripped of endogenous uPA and treated with or without single chain uPA (10 nM) for 10 min (see Experimental Procedures). Cell lysate was incubated with anti-EGFR (mAb 225) or control IgG antibodies, and the immunoprecipitates were blotted for α5 (top) and total EGFR (bottom).

B: T-HEp3 cells were stripped as in **A** and incubated with or without single chain uPA and with or without 1 μM AG1478 for 10 min. EGFR was immunoprecipitated as in Figure 1D, and blotted for phosphotyrosine (RC-20, top panel) and total EGFR (second panel). Cell lysate protein was analyzed for P-ERK (third panel) and ERK (bottom panel) by direct IB.

C: T-HEp3 cells treated with anti-uPAR antibody (R2), isotype matched IgG (IgG), or medium alone (DB) were plated on FN or PLL. EGFR and P-EGFR were determined as in **B**.

the role of EGFR as a downstream effector of the uPA/uPAR induced signal to ERK, uPAR-rich T-HEp3 cells were "acid-stripped" to remove endogenous uPA and treated with 10 nM pro-uPA for 10 min. We first examined whether this treatment affected the integrin/EGFR association. The result in Figure 7A shows that binding of uPA to uPAR strongly increased the α5/EGFR association. In a similar experimental setup, the effect of uPA on EGFR and ERK activation was examined. This treatment induced both EGFR and ERK activation (Figure 7B). Moreover, while the EGFR inhibitor AG1478 did not affect the basal levels of active ERK, it completely blocked uPA-stimulated ERK phosphorylation (Figure 7B). Similar results were obtained using the truncated dominant negative mutant of EGFR (EGFRCD533) (results not shown), suggesting that EGFR kinase activity and dimerization are required for ERK activation by uPA/uPAR. To independently test this idea, we tested whether an anti-uPAR antibody that we previously showed to disrupt uPAR/integrin interaction and reduce the signal to ERK in T-HEp3 cells (Aguirre Ghiso et al., 1999) would reduce EGFR phosphorylation. T-HEp3 cells were preincubated either with anti-uPAR antibody or with preimmune IgG, allowed to adhere to FN, and then lysed and immunoprecipitated with anti-EGFR antibody. The immunoprecipitates were tested by Western blotting for EGFR and phospho-EGFR content. As shown (Figure 7C), disruption of uPAR/α5β1 association by anti-uPAR antibody strongly reduced the extent of EGFR-phosphorylation. Similar reduction in EGFR phosphorylation was obtained with HT1080 cells treated with R2 antibody (results not shown).

Overall, our results indicate the existence of a functional link between the uPA-induced integrin activation by uPAR and the FN-induced activation of EGFR. We tested the effect of uPAR/α5β1/EGFR complex disruption on tumor growth in vivo by affecting two individual targets. Assuming that the ERK activating signal required for in vivo growth is uPAR-initiated and EGFR-mediated, theoretically, the disruption of any one of the components should inhibit tumor growth. We used uPAR/integrin disrupting treatment with anti-uPAR antibody (Figure 7C and Aguirre Ghiso et al., 1999) and the EGFR-kinase inhibitor AG1478, individually or together, to pretreat the T-HEp3 cells prior to their inoculation on the CAM. Cells preincubated with IgG served as positive control for tumor growth. Each of the 5 CAMs per group received 5×10^5 cells, and 3 days postinoculation, the inoculated areas of CAMs were excised and dissociated with collagenase, and the tumor cells were counted. The results in Figure 8 show that treatment with anti-uPAR antibody was more efficient in reducing tumor cell growth than the AG1478 treatment, possibly because it affects the very early interaction between the inoculated cell and the FN-containing ECM of CAM. Treatment with the inhibitor was less effective, possibly because its influence is more transient. The combined treatment was the most efficient, allowing only 0.5 population doublings in 3 days.

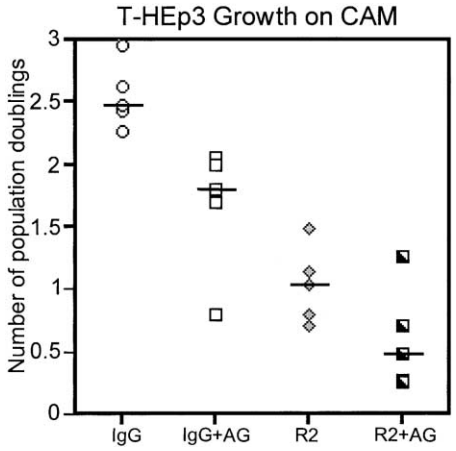

Figure 8. The effect of anti-uPAR antibody, EGFR kinase inhibitor AG1478, and the combination of the two on T-HEp3 cells growth on CAM

T-HEp3 cells pretreated for 24 hr with 1 μM AG1478 (AG) or untreated were incubated with anti-uPAR (R2, 10 μg/ml) or isotype-matched IgG 30 min prior to inoculation on the CAM. The CAMs were collected after 72 hr and tumor cells counted (see Experimental Procedures). Number of population doublings is plotted. The median population doubling for each treatment is indicated. $P < 0.01$ IgG versus AG, R2, and R2+AG; $P < 0.05$ AG versus R2, R2+AG; $P = 0.0582$ R2 versus R2+AG (although there is observable difference between the last two treatments, values did not reach statistical significance), as determined by Mann-Whitney test.

We suspect that the lack of complete growth inhibition by the individual treatments and the increased effect of the combined treatment reflect the transient nature of the interventions and not the presence of separate signaling pathways from uPAR and from EGFR to ERK.

Discussion

The findings presented in this manuscript lead to the unexpected conclusion that uPAR, a GPI-linked protease receptor, can influence the state of phosphorylation and signaling activity of the membrane receptor tyrosine kinase, EGFR, and that this effect is independent of EGFR ligands and does not require high EGFR expression. Our previously published and current data, obtained mainly using HEp3 human carcinoma cells, lead us to the following model: in cells with low uPAR, which are dormant in vivo (Aguirre Ghiso et al., 1999; Yu et al., 1997), the α5β1 integrin exists in an inactive state and associates poorly with EGFR, and in spite of its high expression, both under basal conditions or after cell adhesion to FN, EGFR is not phosphorylated. In cells with high uPAR (T-HEp3, LK25, and D-HEp3 engineered to reexpress uPAR), this receptor, in presence of uPA, interacts frequently with and activates α5β1, leading, in the presence of FN, to the formation of a multiprotein complex that contains at the very least FAK and EGFR, and that subsequently causes robust ERK activation. In contrast, in cells expressing very low levels of uPAR, the very small fraction of EGFR that associates with the integrin is not phosphorylated. Inhibition of EGFR-kinase appears to extinguish the entire uPAR-induced signal to ERK indicating the important role of EGFR in mediating this signal.

Does high uPAR expression have a functional role in EGFR activation?

Specific ligands working through paracrine or autocrine loops are well-established activators of EGFR (Schlessinger, 2000), but we found no indication that ligand expression could explain the difference in EGFR activation (Figure 2). It was previously shown that following integrin/matrix interaction, the EGFR can become phosphorylated and can activate ERK (Moro et al., 1998). The authors concluded that the activation, which represented only a fraction of that achieved by EGF treatment, occurred only in cells with abundant EGFR expression and even then, if EGF or serum was absent, the activation of ERK and entry into S phase did not result in cell division. In contrast, in the D-HEp3 and AS24 cells, which had high EGFR expression, the EGFR was not activated, while in the T-HEp3 and LK25 cells, with low EGFR but high uPAR, it was strongly activated in the basal state and induced by adhesion to FN (Figure 1), but not substantially further increased by addition of EGF (results not shown). Similarly, using specific antibodies, we found no evidence that either a constitutively active truncated receptor, EGFRvIII, or EGFR heterodimerization with other members of the erbB family (erbB2, 3, or 4), were responsible for its activation (results not shown).

While clues implicating known mechanisms of EGFR activation were not found, the experimental results pointed to uPAR as having a functional role. First, the fraction of integrin-associated EGFR, and that of EGFR-associated integrin, was found to be ~10-fold greater in cells overexpressing uPAR. This was true both for the parental T-HEp3 cells, where the overexpressed uPAR constitutively associates with the α5β1 integrin, and for D-HEp3 cells overexpressing uPAR by transfection (Figure 5B). In addition, in HT1080 fibrosarcoma cells transfected with uPAR-antisense under tetracycline inducible promoter, down-regulation of uPAR expression by removal of tetracycline (tet-off) reduced the integrin/EGFR association (results not shown). Likewise, active EGFR colocalized with the β1 integrin (Figure 3D), and β1-integrin colocalized with uPAR when the latter was overexpressed (Aguirre Ghiso et al., 2001). Finally, the uPAR structure/function analysis showed that FN-dependent EGFR phosphorylation was strongest in D-HEp3 cells transfected with full length uPAR, and even more so in cell transfected with the uPARnc in which domain D1 cannot be cleaved by proteases (Figure 5F). EGFR phosphorylation in D-HEp3 cells transfected with the truncated D2D3 mutant was marginal. These results show that uPAR can activate EGFR, and that D1 per se, or the effect its presence has on uPAR conformation, is necessary for the initiation of the signal that leads to EGFR activation. This is supported by published results showing that D1 may be required for uPAR interaction with integrins (Montuori et al., 1999, May et al., 2000).

Regulation by uPAR of integrin activity

Until the structures and sites of interaction of uPAR, integrin, and EGFR, and very likely other proteins, are solved, the precise mechanism of signal propagation from uPAR to ERK cannot be conclusively established. It appears, however, that uPAR may activate the α5β1 integrin by a mechanism similar to that invoked for integrin activation by Mn^{2+} or activating antibodies such as TS2/16 (Bazzoni et al., 1995, 1998). Brief incubation of low uPAR, D-HEp3 cells with 1.5 mM Mn^{2+} or with TS2/16 antibodies induced a degree of FN-dependent EGFR phosphor-

ylation similar to transfection with uPAR (Figure 5). Functional modulation of β2 and β3 integrins by uPAR has been described (Todd and Petty, 1997; Ossowski and Aguirre Ghiso, 2000). Others have shown that EGFR activation by FN was dependent on high EGFR levels (Moro et al., 1998) or the mere presence of α5β1 integrins (Kuwada and Li, 2000). It appears that in some cells α5β1 is active, or becomes activated, when exposed to the ligand. In contrast, we found that in the absence of uPAR in D-HEp3, AS24, and HT1080 cells upon uPAR downregulation, the integrins are inactive, such that under conditions that allow signaling of T-HEp3 cells, plating these cells on FN does not activate integrin signaling. However, increasing uPAR expression activates α5β1 integrins as evidenced by their ability to organize surface FN-fibrils, increase adherence to FN (Aguirre Ghiso et al., 1999, 2001), activate EGFR, and initiate a signal transduction pathway to ERK. Moreover, we have previously shown that addition of soluble uPAR to D-HEp3 and AS24 cells caused rapid ERK activation, suggesting that it is the physical interaction between these two proteins that changes integrin function (Aguirre Ghiso et al., 1999). Previous studies have shown that ligand binding or aggregation of integrins facilitates their interaction with growth factor receptors producing synergistic or additive signaling at the MAPK level (Miyamoto et al., 1996; Kuwada and Li, 2000). The possibility exists that uPAR may affect the membrane distribution of integrins and EGFR and that in some cells, in which integrin function may be affected by transdominant inhibitors such as other integrins or tetraspanins (Diaz-Gonzalez et al., 1996; Hemler, 1998; Hodivala-Dilke et al., 1998), exposure to a ligand may be insufficient to relieve this inhibition.

EGFR is the mediator of the uPAR-induced signal to ERK

Our results linking uPAR overexpression with EGFR and ERK activation prompted the question of the role of EGFR as the mediator of the uPAR-induced signal to ERK. The intracellular domain of EGFR has kinase activity that is required for autophosphorylation and phosphorylation of EGFR substrates (Ullrich et al., 1984) and is inhibited by specific inhibitors such as AG1478, a tyrphostin (Daub et al., 1996). As expected, the FN-induced EGFR phosphorylation was almost completely blocked in T-HEp3 cells treated with AG1478 or in T-HEp3 cells expressing the truncated, dominant negative EGFR. More importantly, ERK activation was reduced to basal levels by both EGFR inhibitory approaches. Two additional experimental results linked uPAR function to EGFR activation of ERK. First, in cells depleted of endogenous uPA, treatment with exogenous pro-uPA increased the integrin/EGFR association. Second, treatment with anti-uPAR antibody, which causes "deactivation" of integrin and loss of active ERK (Aguirre Ghiso et al., 2001), almost completely blocked FN-induced EGFR phosphorylation. These results place the EGFR downstream of uPAR-induced integrin activation and identify it as a mediator of uPAR-induced ERK activity. Moreover, the results indicate that both kinase activity and, probably, dimerization of EGFR are required for mediation of the uPA/uPAR signal to ERK.

Is FAK involved in uPAR induced EGFR and ERK activation?

We showed that in addition to high uPAR expression, active and properly localized FAK (Aguirre Ghiso, 2002) is required for maximal FN-induced EGFR and ERK activation. This conclusion is based on the observations that phosphorylated FAK, and other phosphoproteins, were associated with EGFR only in cells with high uPAR growing in vivo or following adhesion to FN (Figure 6A and 6B), and that expression of FRNK in T-HEp3 cells drastically reduced the integrin/EGFR association and FN-induced EGFR activation. We previously showed that overexpression of uPAR increased the phosphorylation of FAK on Tyr-397, increased phospho-Src association with FAK, and caused Ras and ERK activation (Aguirre Ghiso, 2002), and that FRNK inhibited Ras and ERK activation in T-HEp3 cells. This, combined with the FRNK-mediated EGFR inhibition shown here, suggests that similar to the integrin and growth factor-induced EGFR activation, FAK may also be bridging the uPAR-induced, ligand independent EGFR activation of the classical EGFR-Ras-ERK mitogenic pathway. The fact that FRNK displaces FAK from focal contacts in T-HEp3 cells and reduces FAK, Ras, and ERK activation suggests that as reported by Sieg et al. (2000), structural integrity of EGFR-FAK and, in our case, uPAR/α5β1 must be present to propagate the mitogenic signal from FN and uPA.

The consequence of EGFR-activation by uPAR to tumor growth

We do not know the precise mechanism of EGFR activation in the multimeric complex we describe here. However, the fact that integrin aggregation can induce EGFR phosphorylation (Miyamoto et al., 1996) suggests that uPAR may serve this function in HEp3 cells, and that this may result in the assembly of a large multimolecular complex of phosphorylated proteins. The presence of high uPAR maintains high ERK activity through a pathway that appears to have similarity to the "classical" ligand-growth receptor induced pathway (Schlessinger, 2000), but requires no ligand for in vivo tumor cell proliferation. The conclusion that EGFR ligand plays no role in in vivo proliferation of these cells is further reinforced by the observation that D-HEp3 cells, which are fully responsive to EGF (Figure 2C), had no active EGFR, and no association with phosphorylated proteins, when maintained in vivo (Figure 6A). Although we have not yet performed an extensive screen of cell lines or primary tumors for the presence of this signaling complex, we have some indications that it is not limited to HEp3 and HT1080 cells. If found to be true for other cancers, this conclusion may have profound importance for cancer therapy, since the uPAR-FN-induced pathway of EGFR activation would not be sensitive to blocking of the EGFR-ligand interaction. In support of this conclusion, CaCo colon carcinoma cells transfected with α5-integrin and plated on FN were not growth inhibited by function-blocking anti-EGFR monoclonal antibody 225 (Kuwada and Li, 2000). These cells do not express detectable levels of uPAR (results not shown), suggesting that other pathways of integrin-induced EGFR activation may also be resistant to inhibition by EGFR antagonists. Our results unveil a model whereby highly malignant human carcinoma cells, through overexpression of uPAR, are able to subvert and utilize a tightly regulated EGFR pathway to gain matrix-derived proliferative advantage.

Experimental procedures

Cell lines, transfection, and culture conditions

Human epidermoid carcinoma HEp3 (T-HEp3) (Toolan, 1954) serially passaged on the chorioallantoic membrane (CAM) of 9- to 10-day-old chick

embryos (Specific Pathogen-Free Avian Supply, North Franklin, CT) was used as a source of tumorigenic cells. The source of "spontaneous" dormant tumor cells (D-HEp3) was HEp3 cells passaged in culture 100–170 times (Ossowski and Reich, 1980), with ~20% of uPAR found in tumorigenic cells (Aguirre Ghiso et al., 1999). LK25 (high uPAR, tumorigenic) is a clone of HEp3 cells transfected with vector LK444; AS24 (uPAR ~20% of T-HEp3, dormant) is a clone of T-HEp3 transfected with LK444 vector expressing antisense uPAR-mRNA (Yu et al., 1997; Aguirre Ghiso et al., 1999). T-HEp3 expressing FAK-related-non-kinase (FRNK) or vector transfected control were as described previously (Aguirre Ghiso, 2002). Transfections were performed with FuGENE™ (Roche, Indianapolis, IN) under recommended conditions.

Expression constructs of uPAR and uPAR mutants were generated as follows. Full-length uPAR-cDNA in pCDM8 (Kook et al., 1994) was subcloned in the Xho1 site of pBS-SK+ (Stratagene, La Jolla, CA) (generating pBS-uPAR). For wild-type uPAR, full-length cDNA fragment of uPAR was spliced out of pBS-uPAR using HindIII. The noncleavable uPAR mutant (protease cleavage sites in the domain 1 and 2 linker region abolished) was prepared by mutating R83K, Y87C, R89K, and R91K. From pBS-uPAR, two overlapping PCR fragments amplified by 5′-GAGCTGCCCAAGCTTCATGGGTC-3′ with 5′-GGAATAGGTACCAGCCTTGCCAGA-3′ and 5′-TGGCCGGGCT GGTACCTGTTCC-3′ with 5′-GGGATTTCAAGCTTAGGTCCAGAG-3′ primers, spliced together using a novel Kpn1 site at codon 85 generating a template containing R83K and Y87C mutations, were subcloned into pCDNA3.1-Hyg (Invitrogen, Carlsbad, CA). Using the resulting template, two overlapping PCR fragments containing R89K and R91K mutations, amplified by 5′-GAGCTGCCCAAGCTTCATGGGTC-3′ with 5′-GCATTCGAGGTACTT GCTTTTGGAAC-3′ and 5′-GTTCCAAAAGCAAGTACCTCGAATGC-3′ with 5′-GGGATTTCAAGCTTAGGTCCAGAG-3′ primers, were spliced together using a Taq 1 site. For the mutant expressing only domains 2 and 3 of uPAR (D2D3), sequence encoding domain one was removed, thereby joining the signal sequence with domains 2 and 3. From pBS-uPAR, a 100 bp PCR fragment containing the signal sequence, amplified by 5′-GAGCTGCCCAA GCTTCATGGGTC-3′ with 5′-ACTGCATGCACTCGAGGCCCCAA-3′ primers, was ligated 5′ of the cDNA of D2D3, which was spliced out of pBS-uPAR with 5′ Taq1 and 3′ HindIII cuts. The resulting fragments of wild-type uPAR, noncleavable uPAR, and D2D3 were cloned nondirectionally in the HindIII site of pCDNA3.1-Hyg. The correct orientation was verified by restriction mapping after Pst1 digestion and sequencing (GeneWiz, New York, NY). D-HEp3 cells transfected with the uPAR constructs in FuGENE™ were selected with hygromycin (Clontech, Palo Alto, CA) (100 μg/ml) and maintained in 100 μg/ml hygromycin. uPAR expression was determine in pooled clones by immunoblot analysis (see Figure 5E and Aguirre Ghiso, 2001).

All cells grown in culture were maintained in DMEM with 10% FBS with or without appropriate concentration of drug.

RT-PCR and Northern analysis

Total RNA from ~1 × 10^7 T-HEp3, D-HEp3, LNCaP (positive control for EGF), MCF-7 (positive control for HB-EGF), and MDA231 (positive control for TGF-α and β-cellulin) serum-starved for 24 hr was extracted using an Ultraspec RNA isolation system (Biotecx Laboratories, Houston, TX). For RT-PCR, cDNA was made from total RNA using SuperScript™ First-Strand Synthesis System (Life Technologies, Rockville, MD). PCR amplification was performed with the following primers: 5′-ACCAGAAGTCCTGAAACTAAT-3′ and 5′-TCTCTCACACCTTGCTCCAAT-3′ for β-cellulin; 5′-TCTCAACACAT GCTAGTGGCTGAAATCATG-3′ and 5′-TCAATATACATGCACACACCAT CATGGAGGC-3′ for EGF; and 5′-TCATCATCTCTGCCCCCTCT-3′ and 5′-TCCGACGCCTGCTTCACCAC-3′ for GAPDH. 300 bp PCR-amplified fragment of human amphiregulin, for PCR positive control, and associated primers were provided by Dr. Jonathan Licht (Mount Sinai School of Medicine). PCR primers for TGF-α were provided by Dr. Paolo Fedi (Mount Sinai School of Medicine).

For Northern blot analysis, ^{32}P-labeled TGF-α, HB-EGF, and GAPDH probes were generated by random priming (DECA prime II DNA labeling kit, Ambion, Austin, TX) of plasmid DNA for TGF-α (from ATCC TGF-1-10-925 PLASMID 59950) and PCR generated fragments for HB-EGF and GAPDH. 50 μg of total RNA was transferred to Hybond nylon membranes (Amersham Life Sciences, Buckinghamshire, UK), and processed as previously described (Yu et al.) for signal development using ^{32}P-labeled probes. The signal was developed using XOMAT film (Kodak, Rochester, NY) with intensifying screens after exposure for 4–24 hr at −80°C.

Growth of control and treated tumor cells on CAMs

Subconfluent cell monolayers (see figure legends for details) treated with 1 μM AG1478 (Calbiochem, San Diego, CA) or left untreated for 24 hr in serum-free media were detached with 2 mM EDTA in PBS, washed, and inoculated on the CAMs (5 × 10^5 cells per CAM) of 9- to 10-day-old chick embryos. In some experiments, prior to inoculation, the cells were incubated for 30 min at 37°C with anti-human uPAR mAb (R2; 10 μg/ml) (kindly provided by Dr. Michael Ploug, Finsen Laboratory), anti-EGFR mAb (mAb 225; 10 μg/ml), or isotype matched IgG (Sigma Chemical, St. Louis, MO) as control. At indicated times postinoculation, CAMs were excised, enzymatically dissociated, and tumor cells in single-cell suspensions were counted (Aguirre Ghiso et al., 1999). All antibodies used in vivo or in culture were free of azide. The antibodies used in vivo had <24 pg/ml endotoxin measured by the PyrogenPlus test from Biowhittaker (Walkersville, MD).

To analyze EGFR phosphorylation and complex formation in vivo, 2 × 10^5 T-HEp3 and 1 × 10^6 D-HEp3 were inoculated on the CAM. Following 7 days of growth in vivo, tumors were collected in 1% NP-40 lysis buffer (1% NP-40, 50 mM Tris-HCl, 150 mM NaCl, 1 mM orthovanadate, 1 mM NaFl, 200 KIU/ml aprotinin, 1 μg/ml leupeptin, 1 μg/ml pepstatin, 1 mM PMSF, 5 mM EDTA [pH 8]), snap-frozen in liquid nitrogen, thawed, homogenized, kept on ice for 1 hr, cleared of debris by centrifugation, and immunoprecipitated for EGFR as described below. CAM tissue was used as controls for the specificity of the anti-human EGFR mAb 225.

FACS analysis

Cells were detached with 2 mM EDTA in PBS and resuspended in cold PBS with Ca^{2+}, Mg^{2+}, and 1% FBS at 10^7 cells/ml. Anti-EGFR mAb225, or isotype matched IgG, was added to 5 × 10^5 cells at 10 μg/ml, incubated at 4°C for 30 min, and after two washes, incubated for 30 min at 4°C with FITC-conjugated goat anti-mouse (1 μg/ml) IgG. The cells were washed twice, fixed in 5% formaldehyde in PBS, and analyzed in FACS®Calibur (Becton Dickinson) using 488 nm excitation wavelength.

Immunoprecipitation (IP) and immunoblotting (IB)

Subconfluent monolayers were washed with PBS and lysed with 1% NP-40 (for IP) or RIPA (1% Triton X 100, 140 mM NaCl, 10 mM Tris, 0.025% NaN3, 0.1% SDS) (for IB) buffers with protease and phosphatase (1 mM orthovanadate, 1 mM NaFl) inhibitors. Protein concentration was determined by BioRad Protein Assay (BioRad, Hercules, CA). For direct IB, 20 to 50 μg of total protein was analyzed. For IP, total protein (0.5 to 1.5 mg) was precleared with protein-G-agarose for 1 hr at 4°C and the supernatant was incubated with antibodies against human EGFR (mAb 225, from hybridoma obtained from ATCC, Rockville, MD; Mouse Ab5, Calbiochem, San Diego, CA), β1 integrin (mAb TS2/16, Pierce Endogen, Rockford, IL), and α5β1 integrin (mAb VLA5, Chemicon International, Temecula, CA) overnight at 4°C, and after washing the immunoprecipitates were analyzed by IB. SDS-PAGE and IB were performed as previously described (Aguirre Ghiso et al., 1999) using antibodies against ERK1/2 (mAb MK12), active-EGFR (mAb 74), FAK (mAb 77), phosphotyrosine (PY-20 and RC-20) (all from Transduction Laboratories Lexington, KY), human EGFR (rabbit polyclonal anti-EGFR, provided by Dr. Paolo Fedi, Mount Sinai School of Medicine; or mAb 14, NeoMarkers, Union City, CA), phospho-ERK1/2 (mAb E4, Santa Cruz Biotechnology Santa Cruz, CA), uPAR (R2), β1 integrin (anti-CD29, NeoMarkers), or α5 integrin (anti-α5 rabbit polyclonal antibody, Chemicon). When necessary, the membranes were stripped with stripping buffer (62.5 mM Tris [pH 6.8], 2% SDS, 100 mM β-mercaptoethanol) for 30 min at 50°C, and washed with TBST. When indicated, the bands were quantitated by laser densitometry using GelScan XL (Pharmacia, Upsala, Sweden), the optical density units were normalized to controls and, graphs generated with CA-Cricket Graph III.

Immunofluorescence microscopy

Cells grown on coverslips were fixed and processed as previously described (Aguirre Ghiso et al., 2001).Cells were stained with anti-β1-integrin (AIIB2, 4 μg/ml, Developmental Study Hybridoma Bank, University of Iowa, Ames, IA) and anti-activated-EGFR (mAb 74, 2 μg/ml) antibodies in 0.1% BSA/PBS, or with vehicle alone. After washing and blocking, secondary antibody (FITC-conjugated anti-rat IgG at 1:400, Sigma; AlexaRed-conjugated anti-

mouse IgG at 1:1000, Molecular Probes, Eugene, OR) in 0.1% BSA/PBS containing DAPI was added. Standard epifluorescence was captured with an Axioskop epifluorescence photomicroscope (Zeiss, Oberkochen, Germany) and confocal microscopy was performed using a TCS SP spectral confocal laser scanning microscope (Leica Microsystems, Heidelberg, Germany).

Fibronectin and uPA stimulation

Subconfluent cell monolayers (see below for specific conditions and treatments) were serum-starved for 24 hr, detached with 2 mM EDTA, and plated on plastic dishes precoated for 24 hr in 4°C with 10 μg/ml human fibronectin (FN) or poly-lysine (PLL) (Sigma) as controls. In some experiments, T-HEp3 were pretreated for 20 min with 10 μg/ml CRM197 and plated in the presence of 10 μg/ml CRM197, for 15 min with 1 μM AG1478 and plated in the presence of 1 μM AG1478, or were transiently transfected for 48 hr with vector expressing CD533-EGFR, dominant-negative EGFR (provided by Dr. Axel Ullrich, Max Planck Institute), and plated on FN or PLL. To test the activation of $\alpha5\beta1$, D-HEp3 cells were plated in medium with 1.5 mM $MnCl_2$ or were preincubated for 30 min at 37°C with 10 μg/ml TS2/16 or isotype-matched IgG and used to determine EGFR activation. Disruption of the uPAR/integrin complex in T-HEp3 cells was achieved by incubation of the cells with 10 μg/ml anti-uPAR R2 or isotype-matched IgG for 30 min at 37°C prior to plating. D-HEp3 cells transfected with wild-type and mutant uPAR, or T-HEp3 transfected with vector or vector expressing FRNK were plated on FN or PLL. After 20 min, adherent cells were washed with PBS, lysed with 1% NP-40 or RIPA buffers with protease and phosphatase inhibitors, and analyzed by IP or direct IB. For uPA treatment, subconfluent monolayers of T-HEp3 cells were serum-starved for 24 hr, preincubated for 15 min with or without 1 μM AG1478, acid-stripped of uPAR bound uPA for 3 min (using cold 0.05 M glycine-HCl in 0.1 M NaCl [pH 3]), and neutralized using 0.5 M Tris-HCl (pH 7.8) and incubated for 10 min with 10 nM single chain uPA (scuPA) (provided by Dr. Jack Henkin, Abbott Laboratories) in the presence of 200 KIU/ml aprotinin (to inhibit protease-dependent effects of uPA) with or without AG1478. Cells were lysed with 1% NP-40 with protease and phosphatase inhibitors and analyzed by IP or direct IB.

Acknowledgments

We thank Drs. Rafael Mira y Lopez and George Acs for critical reading of the manuscript, Dr. Inigo Santamaria Ruiz de Azua for preparation of the uPAR-mutant expression vectors, and Dr. Samuel Waxman for continuous encouragement and support. We gratefully acknowledge the gift of the following reagents: monoclonal anti-uPAR antibody (R2) from Dr. Michael Ploug (Finsen Laboratory, Copenhagen DK); rat monoclonal anti $\alpha5\beta1$ antibody (AIIB2) from Dr. Caroline Damsky (University of California, San Francisco, CA); CD533 from Dr. Axel Ullrich (Max Planck Institute, Germany); single chain uPA from Dr. Jack Henkin (Abbott Laboratories, Abbot Park, IL); TGF-α primers and rabbit polyclonal anti-EGFR antibody from Dr. Paolo Fedi (Mount Sinai School of Medicine, New York, NY); amphiregulin DNA and primers from Dr. Jonathan Licht. Confocal laser scanning microscopy was supported with funding from the National Science Foundation Major Research Instrumentation Grant (DBI9724504) of the Mount Sinai School of Medicine Microscopy Center. This work was supported by U.S. Public Health Service Research Grant (CA-40758) (L.O.), NIH/MSSM Medical Scientist Training Program and NCI predoctoral training grant (CA78207) (D.L.), The Charles H. Revson Foundation (J.A.A.G.) and The Samuel Waxman Cancer Research Foundation.

Received: March 28, 2002
Revised: May 22, 2002

References

Aguirre Ghiso, J.A. (2002). Inhibition of FAK signaling activated by urokinase receptor induces dormancy in human carcinoma cells in vivo. Oncogene *21*, 2513–2524.

Aguirre Ghiso, J.A., Kovalski, K., and Ossowski, L. (1999). Tumor dormancy induced by downregulation of urokinase receptor in human carcinoma involves integrin and MAPK signaling. J. Cell Biol. *147*, 89–104.

Aguirre Ghiso, J.A., Liu, D., Mignatti, A., Kovalski, K., and Ossowski, L. (2001). Urokinase receptor and fibronectin regulate the ERK(MAPK) to p38(MAPK) activity ratios that determine carcinoma cell proliferation or dormancy in vivo. Mol. Biol. Cell *12*, 863–879.

Andreasen, P.A., Kjøller, L., Christensen, L., and Duffy, M.J. (1997). The urokinase-type plasminogen activator system in cancer metastasis: a review. Int. J. Cancer *72*, 1–22.

Bazzoni, G., Shih, D.T., Buck, C.A., and Hemler, M.E. (1995). Monoclonal antibody 9EG7 defines a novel beta 1 integrin epitope induced by soluble ligand and manganese, but inhibited by calcium. J. Biol. Chem. *270*, 25570–25577.

Bazzoni, G., Ma, L., Blue, M.L., and Hemler, M.E. (1998). Divalent cations and ligands induce conformational changes that are highly divergent among beta1 integrins. J. Biol. Chem. *273*, 6670–6678.

Bissell, M.J., Weaver, V.M., Lelievre, S.A., Wang, F., Petersen, O.W., and Schmeichel, K.L. (1999). Tissue structure, nuclear organization, and gene expression in normal and malignant breast. Cancer Res. *59*, 1757–1763.

Cary, L.A., and Guan, J.L. (1999). Focal adhesion kinase in integrin-mediated signaling. Front. Biosci. *4*, D102–D113.

Daub, H., Weiss, F.U., Wallasch, C., and Ullrich, A. (1996). Role of transactivation of the EGF receptor in signalling by G-protein- coupled receptors. Nature *379*, 557–560.

Diaz-Gonzalez, F., Forsyth, J., Steiner, B., and Ginsberg, M.H. (1996). Trans-dominant inhibition of integrin function. Mol. Biol. Cell *7*, 1939–1951.

Giancotti, F.G., and Ruoslahti, E. (1999). Integrin signaling. Science *285*, 1028–1032.

Goishi, K., Higashiyama, S., Klagsbrun, M., Nakano, N., Umata, T., Ishikawa, M., Mekada, E., and Taniguchi, N. (1995). Phorbol ester induces the rapid processing of cell surface heparin-binding EGF-like growth factor: conversion from juxtacrine to paracrine growth factor activity. Mol. Biol. Cell *6*, 967–980.

Hemler, M.E. (1998). Integrin associated proteins. Curr. Opin. Cell Biol. *10*, 578–585.

Hodivala-Dilke, K.M., DiPersio, C.M., Kreidberg, J.A., and Hynes, R.O. (1998). Novel roles for alpha3beta1 integrin as a regulator of cytoskeletal assembly and as a trans-dominant inhibitor of integrin receptor function in mouse keratinocytes. J. Cell Biol. *142*, 1357–1369.

Hoyer-Hansen, G., Ronne, E., Solberg, H., Behrendt, N., Ploug, M., Lund, L.R., Ellis, V., and Dano, K. (1992). Urokinase plasminogen activator cleaves its cell surface receptor releasing the ligand-binding domain. J. Biol. Chem. *267*, 18224–18229.

Keely, P., Parise, L., and Juliano, R. (1998). Integrins and GTPases in tumour cell growth, motility and invasion. Trends Cell Biol. *8*, 101–106.

Kook, Y.H., Adamski, J., Zelent, A., and Ossowski, L. (1994). The effect of antisense inhibition of urokinase receptor in human squamous cell carcinoma on malignancy. EMBO J. *13*, 3983–3991.

Kuwada, S.K., and Li, X. (2000). Integrin alpha5/beta1 mediates fibronectin-dependent epithelial cell proliferation through epidermal growth factor receptor activation. Mol. Biol. Cell *11*, 2485–2496.

May, A.E., Neumann, F.J., Schomig, A., and Preissner, K.T. (2000). VLA-4 (alpha4/beta1) engagement defines a novel activation pathway for beta2 integrin-dependent leukocyte adhesion involving the urokinase receptor. Blood *96*, 506–513.

Mitamura, T., Higashiyama, S., Taniguchi, N., Klagsbrun, M., and Mekada, E. (1995). Diphtheria toxin binds to the epidermal growth factor (EGF)-like domain of human heparin-binding EGF-like growth factor/diphtheria toxin receptor and inhibits specifically its mitogenic activity. J. Biol. Chem. *270*, 1015–1019.

Miyamoto, S., Teramoto, H., Gutkind, J.S., and Yamada, K.M. (1996). Integrins can collaborate with growth factors for phosphorylation of receptor tyrosine kinases and MAP kinase activation: roles of integrin aggregation and occupancy of receptors. J. Cell Biol. *135*, 1633–1642.

Montuori, N., Rossi, G., and Ragno, P. (1999). Cleavage of urokinase receptor regulates its interaction with integrins in thyroid cells. FEBS Lett. *460*, 32–36.

Moro, L., Venturino, M., Bozzo, C., Silengo, L., Altruda, F., Beguinot, L., Tarone, G., and Defilippi, P. (1998). Integrins induce activation of EGF receptor: role in MAP kinase induction and adhesion-dependent cell survival. EMBO J. *17*, 6622–6632.

Nicholson, R.I., Gee, J.M., and Harper, M.E. (2001). EGFR and cancer prognosis. Eur. J. Cancer *37* (*Suppl 4*), S9–S15.

Ossowski, L., and Aguirre Ghiso, J.A. (2000). Urokinase receptor and integrin partnership: coordination of signaling for cell adhesion, migration and growth. Curr. Opin. Cell Biol. *12*, 613–620.

Ossowski, L., and Reich, E. (1980). Loss of malignancy during serial passage of human carcinoma in culture and discordance between malignancy and transformation parameters. Cancer Res. *40*, 2310–2315.

Redemann, N., Holzmann, B., von Ruden, T., Wagner, E.F., Schlessinger, J., and Ullrich, A. (1992). Anti-oncogenic activity of signalling-defective epidermal growth factor receptor mutants. Mol. Cell. Biol. *12*, 491–498.

Ruoslahti, E. (1999). Fibronectin and its integrin receptors in cancer. Adv. Cancer Res. *76*, 1–20.

Schlessinger, J. (2000). Cell signaling by receptor tyrosine kinases. Cell *103*, 211–225.

Schmitt, M., Wilhelm, O.G., Reuning, U., Kruger, A., Harbeck, N., Lengyel, E., Graeff, H., Gansbacher, B., Kessler, H., Burgle, M., et al. (2000). The urokinase plasminogen activator system as a novel target for tumor therapy. Fibrinolysis Proteolysis *14*, 114–132.

Sieg, D.J., Hauck, C.R., Ilic, D., Klingbeil, C.K., Schaefer, E., Damsky, C.H., and Schlaepfer, D.D. (2000). FAK integrates growth-factor and integrin signals to promote cell migration. Nat. Cell Biol. *2*, 249–256.

Spivak-Kroizman, T., Rotin, D., Pinchasi, D., Ullrich, A., Schlessinger, J., and Lax, I. (1992). Heterodimerization of c-erbB2 with different epidermal growth factor receptor mutants elicits stimulatory or inhibitory responses. J. Biol. Chem. *267*, 8056–8063.

Todd, R.F., 3rd, and Petty, H.R. (1997). Beta 2 (CD11/CD18) integrins can serve as signaling partners for other leukocyte receptors. J. Lab. Clin. Med. *129*, 492–498.

Toolan, H.W. (1954). Transplantable human neoplasms maintained in cortisone-treated laboratory animals: HS#1, H.Ep#1, H.Ep.#2, H.Ep.#3, and H.Emb.#1. Cancer Res. *14*, 660–666.

Ullrich, A., Coussens, L., Hayflick, J.S., Dull, T.J., Gray, A., Tam, A.W., Lee, J., Yarden, Y., Libermann, T.A., Schlessinger, J., et al. (1984). Human epidermal growth factor receptor cDNA sequence and aberrant expression of the amplified gene in A431 epidermoid carcinoma cells. Nature *309*, 418–425.

Wary, K.K., Mariotti, A., Zurzolo, C., and Giancotti, F.G. (1998). A requirement for caveolin-1 and associated kinase Fyn in integrin signaling and anchorage-dependent cell growth. Cell *94*, 625–634.

Yu, W., Kim, J., and Ossowski, L. (1997). Reduction in surface urokinase receptor forces malignant cells into a protracted state of dormancy. J. Cell Biol. *137*, 767–777.